

Surface Science Letters

# Surface electron accumulation in indium nitride layers grown by high pressure chemical vapor deposition

R.P. Bhatta, B.D. Thoms<sup>\*</sup>, M. Alevli, N. Dietz

*Department of Physics and Astronomy, Georgia State University, Atlanta, GA 30303, United States*

Received 30 March 2007; accepted for publication 11 July 2007

Available online 21 July 2007

## Abstract

Surface termination and electronic properties of InN layers grown by high pressure chemical vapor deposition have been studied by high resolution electron energy loss spectroscopy (HREELS). HREEL spectra from InN after atomic hydrogen cleaning show N–H termination with no indium overlayer or droplets and indicate that the layer is N-polar. Broad conduction band plasmon excitations are observed centered at  $3400\text{ cm}^{-1}$  in HREEL spectra with 7 eV incident electron energy which shift to  $3100\text{ cm}^{-1}$  when the incident electron energies are 25 eV or greater. The shift of the plasmon excitations to lower energy when electrons with larger penetration depths are used is due to a higher charge density on the surface compared with the bulk, that is, a surface electron accumulation. These results indicate that surface electron accumulation on InN does not require excess indium or In–In bonds.

© 2007 Elsevier B.V. All rights reserved.

*Keywords:* Electron energy loss spectroscopy; Vibrational spectroscopy; Indium nitride; Hydrogen; Surface structure; Surface electronic phenomena

The physical properties of InN have attracted considerable research interest because of its transport properties such as high electron mobility and saturation velocity making it a promising candidate for use in high-speed devices [1,2]. In addition, InN–GaN–AlN alloys and heterostructures will enable unique optoelectronic devices, operating from near infrared to ultraviolet wavelength regime [1,3]. However, the range of device applications strongly depends on the material properties and quality and on the extent to which indium-rich alloys and heterostructures can be formed [3].

The growth of InN is challenging since InN and indium-rich group III-nitride alloys exhibit a high equilibrium vapor pressure of nitrogen during growth and a low decomposition temperature compared to GaN and AlN. These challenges also lead to difficulties in growing structures containing indium-rich III-nitrides embedded in layers of lower indium content [4]. InN films have been grown by a number

of techniques including metal–organic chemical vapor deposition (MOCVD) and molecular beam epitaxy (MBE) but many of the fundamental electrical and optical properties are still in debate including the correct band gap energy [1,3]. High pressure chemical vapor deposition (HPCVD) has been developed to address these challenges and has been shown to be capable of growing high-quality InN [4–6]. Using HPCVD, stoichiometry controlled InN layers have been grown at temperatures around 1100 K [6].

There have been several reports regarding surface electron accumulation on InN layers. A number of investigations of carrier concentration as a function of film thickness have measured charge accumulation layers with electron densities over the range of  $1.6\text{--}5.1 \times 10^{13}\text{ cm}^{-2}$  [7–9]. Lu et al. [7] also reported ohmic contacts for a number of metals without annealing and suggested that surface electron accumulation due to pinning of the Fermi level above the conduction band minimum was responsible. A series of papers by McConville and coworkers [10–15] report surface electron accumulation as measured by high resolution electron energy loss spectroscopy (HREELS) and X-ray photoemission spectroscopy on MBE-grown InN layers. Colakerol et al. [16] used

<sup>\*</sup> Corresponding author. Tel.: +1 404 4136045; fax: +1 404 4136025.  
E-mail address: [bthoms@gsu.edu](mailto:bthoms@gsu.edu) (B.D. Thoms).

angle-resolved photoemission spectroscopy to observe quantized energy levels in the surface electron accumulation layer on InN films grown by radio frequency plasma-assisted molecular beam epitaxy.

Surface electron accumulation has been reported to be due to a particularly low  $\Gamma$ -point conduction band minimum in both InAs [17] and InN [14]. In the case of InAs, the surface electron concentration is reported to depend on surface reconstruction [17,18]. The carrier concentration of an InN epilayer grown by MOCVD has been altered by exposure to a microwave hydrogen plasma [19]. The changes were suggested as due to the removal of surface contaminants such as oxygen and by the migration of indium clusters to the surface during etching. Indium clusters have been reported to be present in the bulk of InN layers [20,21] and both indium overlayers and droplets have been reported on InN surfaces [22,23]. The influence of In overlayers or droplets on electron accumulation at the InN surface is not yet understood. Segev and Van de Walle [24] have suggested that occupied surface states caused by In–In bonds are the cause of electron accumulation on InN surfaces.

In an earlier HREELS study of HPCVD-grown InN, the authors reported surface N–H termination and concluded that the film was N-polar [25]. The HREELS studies reported here were performed on different HPCVD InN layers grown under different process conditions, which also exhibit N-polarity. We report here surface electron accumulation on an InN layer as observed by HREELS on a surface of known termination with no indium overlayers or droplets.

The results presented here were acquired from an InN layer grown at a temperature of 1120 K, a reactor pressure of 15 bar, and an ammonia to trimethyl-indium precursor ratio of 630 on a HPCVD-grown GaN buffer layer on a sapphire (0001) substrate. Details of the HPCVD reactor, the growth configuration, as well as real-time optical characterization techniques employed have been published elsewhere [4,5]. The spectra reported here were all acquired from the same sample, however similar results were observed from other InN films grown under similar conditions.

The ultrahigh vacuum (UHV) surface characterization system [26] had a base pressure of  $1.8 \times 10^{-10}$  Torr. The InN sample was rinsed with isopropyl alcohol and then attached to a tantalum sample holder using tantalum clips before introduction into the UHV chamber. Sample heating was accomplished by electron bombardment of the back of the tantalum sample holder. Sample temperature was measured with a chromel–alumel thermocouple attached to the mount next to the sample. HREELS experiments were performed in a specular scattering geometry with an incident and scattered angle of  $60^\circ$  from the normal and incident electron energy ranging from 7 eV to 35 eV. An instrumental resolution of  $60 \text{ cm}^{-1}$  was obtained as determined from the elastic peak full width at half maximum.

The surface of the InN sample was first cleaned by bombardment of 1 keV Ar ions at an angle of  $70^\circ$  from

the normal to remove surface carbon contamination from exposure to air during transport to the UHV chamber. When Auger electron spectroscopy showed removal of nearly all surface carbon, the sample was treated using atomic hydrogen cleaning (AHC) [10]. Atomic hydrogen exposures were performed by backfilling the vacuum chamber with hydrogen to a pressure of  $8.4 \times 10^{-7}$  Torr in the presence of a tungsten filament heated to 1850 K. The sample was positioned 20 mm from the filament for 20 min (giving an exposure of 1000 L of  $\text{H}_2$ ) during which time the sample temperature rose to about 350 K due to proximity to the heated filament. After this, the sample was heated to 600 K while remaining in front of the tungsten filament for an additional 20 min (an additional 1000 L of  $\text{H}_2$ ). Auger electron spectroscopy (AES) and HREELS showed that surface carbon and oxygen contaminants had been removed. Low energy electron diffraction (LEED) yielded a hexagonal  $1 \times 1$  pattern over the entire surface of the film using electron energies from 40 to 170 eV indicating good surface order and  $c$ -axis orientation of the InN layer.

HREEL spectra from the AHC-treated InN layer were acquired using a range of incident electron energies and are shown in Fig. 1. In all the spectra, a strong loss feature was observed at  $560 \text{ cm}^{-1}$  which is assigned to Fuchs–Kliener surface phonon excitations in agreement with previous

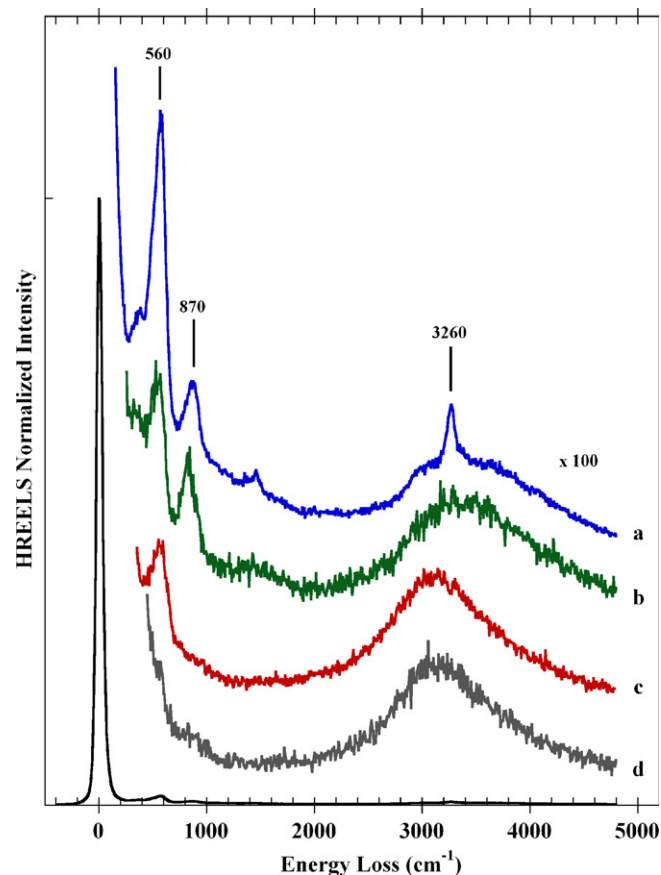


Fig. 1. HREELS from an atomic hydrogen cleaned InN sample. Spectra were acquired in the specular direction with incident electron energies of (a) 7 eV, (b) 15 eV, (c) 25 eV, and (d) 35 eV.

reports [10–15,25]. The HREEL spectrum taken using 7 eV incident electron energy shows surface adsorbate loss features at 870 and 3260  $\text{cm}^{-1}$  due to the bending and stretching vibrations of a surface N–H species [25]. A small peak observed near 1430  $\text{cm}^{-1}$  is assigned to a combination loss of the Fuchs–Kliwer phonon and the N–H bending vibration. With the incident electron energy increased to 15 eV, the intensity of the N–H stretch decreased considerably while the N–H bend was almost unchanged. The difference in the dependence of the intensity of the two peaks on incident energy suggests that different scattering mechanisms are contributing. According to Ibach and Mills [27], the dipole scattering cross-section decreases with the increasing incident energy while the impact scattering cross-section is less predictable and may even increase. Therefore, the excitation of the N–H stretch is attributed primarily to dipole scattering while the N–H bend has a considerable contribution due to impact scattering. As the incident energy is increased further, all modes due to surface vibrations decrease due to reduction in surface sensitivity with an increasing penetration depth of the electrons.

In–H stretching vibrations, typically found between 1650 and 1700  $\text{cm}^{-1}$  [28–31], are not observed in these spectra even with 7 eV incident electron energy. Since hydrogen desorption may occur from indium sites at the 600 K temperature used for AHC, additional room temperature hydrogen atom exposures were performed. HREEL spectra from the room temperature H-dosed surface were unchanged from those shown in Fig. 1 indicating that no reactive indium exists on this surface. The presence of N–H and lack of indium-related vibrations demonstrates N-termination of the surface and implies N-polarity of the film since N-termination would not be expected for In-polar films [32]. Along with the observed  $1 \times 1$  surface order, this also shows that the surface is free of both indium overlayers and droplets.

The observation of an N–H terminated surface free of excess indium differs from the conclusion of several recent reports. An investigation by Draxler et al. [23] using coaxial impact collision ion scattering spectroscopy (CAICISS) determined that metallic In was present on N-polar InN surfaces after cleaning by atomic hydrogen. Piper et al. [22] also concluded that metallic In is sometimes present on the InN surface after AHC based on X-ray photoemission spectroscopy. They assign a component of the In4d peak to In–In bonds. However, the relative intensity of the In–In feature relative to the In–N component and the lack of surface sensitivity due to nearly 1500 eV photon and electron energies suggest that this component is more likely due to bulk indium clusters.

A broad loss feature, with a peak in the range of 3100–3400  $\text{cm}^{-1}$  for different incident electron energies, also appears in each spectrum. Following the assignment of McConville and coworkers [10–15], we attribute these broad features as due to conduction band plasmon excitations. The plasmon peak energy decreases when the incident electron energy is increased.

In general, the shift of the plasmon loss feature in HREEL spectra with incident electron energy may be attributed to three causes: dispersion, the kinematic factor, and variation of the carrier concentration with depth. Froitzheim et al. [33] have reported that if the parallel momentum transfer vector is much smaller than the reciprocal lattice vector then the wave vector dependence of dielectric function  $\epsilon(\omega, q)$  can be ignored. Under the conditions used in this study, the parallel momentum transfer vector is small ( $\leq 0.04 \text{ \AA}^{-1}$ ), so the role of dispersion in the shift of the plasmon peak position can be excluded.

According to Chen et al. [34], if the loss function contains a broad frequency response due to large damping constant,  $\Gamma$ , which is typical for low mobility p-type semiconductors, then the kinematic effects play a role in determining the peak position for incident energies less than 5 eV. Since the present work was performed on an n-type semiconductor of higher carrier mobility ( $\mu \sim 210 \text{ cm}^2/\text{V s}$ ) using incident electron energies of 7–35 eV, the kinematic factor is not important in determining the energy of the plasmon loss feature.

Excluding both the effects of the kinematic factor and dispersion, the shift of the plasmon peak position is attributed to a variation of carrier concentration with depth. As McConville and coworkers [10–15] demonstrated by performing semiclassical dielectric theory simulations, the position of the plasmon peak is related to the surface and bulk plasma frequencies. The shift of the plasmon feature to lower loss energy as the incident electron energy is increased means that the plasma frequency is larger for the surface than for the bulk and indicates an accumulation of electrons on the surface. As seen in Fig. 1, the plasmon peak position shifts most dramatically when the incident electron energy is changed from 15 to 25 eV but there is almost no shift when incident energy changes from 7 to 15 eV or 25 to 35 eV. The shift of the plasmon feature with incident energy is determined by the depth profile of the carrier concentration along with the sampling depth of the electrons. HREEL spectra reported by Mahboob et al. [14] and Veal et al. [15] also show that most of the shift occurs as the incident energy is changed from 15 to 30 eV and this feature is reproduced in their simulations using a four or five layer slab model with an electron concentration that is large at the surface and decreasing deeper into the layer. The HREEL spectra reported here are therefore consistent with a surface electron accumulation layer.

In most of the reports of experimental observations of surface electron accumulation on InN layers neither film polarity nor surface termination is known. Piper et al. [10,13] have reported that the MBE-grown samples on which they observed surface charge accumulation were 75% In-polar and 25% N-polar as determined by CAICISS. Although HREEL spectra were used in a number of cases to study the surface electron accumulation, no surface adsorbate vibrational loss peaks were observed in those studies so surface termination could not be determined. In the present work, HREEL spectra at low incident elec-

tron energy yield N–H surface vibrations, which indicate both the surface termination and film polarity. The intensity of the N–H vibrations, the lack of In–H vibrations even after room temperature atomic hydrogen exposure, and the presence of a  $1 \times 1$  LEED pattern are evidence that no indium was present on the surface. The electron accumulation observed here is therefore not caused by indium droplets, indium overlayers, or isolated In–In dimers on the InN surface. This finding is consistent with the pinning of the surface Fermi level in the conduction band but indicates that In–In bonds are not the only source of surface states in the conduction band.

In summary, InN layers grown by HPCVD and cleaned by atomic hydrogen have been studied by HREELS. Spectra taken with low incident electron energy demonstrated that the surface is N–H terminated and free of indium overlayers and droplets. Spectra acquired as a function of incident energy revealed the presence of a surface electron accumulation. These results strongly suggest that the electron accumulation on InN surfaces is not due to excess indium.

#### Acknowledgement

The authors would like to acknowledge support of this work by GSU-RPE.

#### References

- [1] A.G. Bhuiyan, A. Hashimoto, A. Yamamoto, *J. Appl. Phys.* 94 (2003) 2779.
- [2] S.K. O’Leary, B.E. Foutz, M.S. Shur, L.F. Eastman, *Appl. Phys. Lett.* 88 (2006) 152113.
- [3] K.S.A. Butcher, T.L. Tansley, *Superlattice. Microstruct.* 38 (2005) 1.
- [4] N. Dietz, M. Alevli, V. Woods, M. Strassburg, H. Kang, I.T. Ferguson, *Phys. Stat. Sol. (b)* 242 (2005) 2985.
- [5] V. Woods, N. Dietz, *Mat. Sci. Eng. B* 127 (2006) 239.
- [6] M. Alevli, G. Durkaya, A. Weerasekara, A.G.U. Perera, N. Dietz, W. Fenwick, V. Woods, I. Ferguson, *Appl. Phys. Lett.* 89 (2006) 112119.
- [7] H. Lu, W.J. Schaff, F. Eastman, C.E. Stutz, *Appl. Phys. Lett.* 82 (2003) 1736.
- [8] L.F.J. Piper, T.D. Veal, C.F. McConville, H. Lu, W.J. Schaff, *Appl. Phys. Lett.* 88 (2006) 252109.
- [9] C.S. Gallinat, G. Koblmuller, J.S. Brown, S. Bernardis, J.S. Speck, G.D. Chern, E.D. Readinger, H. Shen, W. Wraback, *Appl. Phys. Lett.* 89 (2006) 032109.
- [10] L.F.J. Piper, T.D. Veal, M. Walker, I. Mahboob, C.F. McConville, H. Lu, W.J. Schaff, *J. Vac. Sci. Technol. A* 23 (2005) 617.
- [11] I. Mahboob, T.D. Veal, L.F.J. Piper, C.F. McConville, H. Lu, W.J. Schaff, J. Furthmüller, F. Bechstedt, *Phys. Rev. B* 69 (2004) 201307, R.
- [12] T.D. Veal, I. Mahboob, L.F.J. Piper, C.F. McConville, H. Lu, W.J. Schaff, *J. Vac. Sci. Technol. B* 22 (2004) 2175.
- [13] L.F.J. Piper, T.D. Veal, I. Mahboob, C.F. McConville, H. Lu, W.J. Schaff, *Phys. Rev. B* 70 (2004) 115333.
- [14] I. Mahboob, T.D. Veal, C.F. McConville, H. Lu, W.J. Schaff, *Phys. Rev. Lett.* 92 (2004) 036804.
- [15] T.D. Veal, L.F.J. Piper, I. Mahboob, H. Lu, W.J. Schaff, C.F. McConville, *Phys. Stat. Sol. (C)* 7 (2005) 2246.
- [16] L. Colakerol, T.D. Veal, H.K. Jeong, L. Plucinski, A. DeMasi, T. Learnmonth, P.A. Glans, S. Wang, Y. Zhang, L.F.J. Piper, P.H. Jefferson, A. Federov, T.C. Chen, T.D. Moustakas, C.F. McConville, K.E. Smith, *Phys. Rev. Lett.* 97 (2006) 237601.
- [17] M. Noguchi, H. Hirakawa, T. Ikoma, *Phys. Rev. Lett.* 66 (1991) 2243.
- [18] L.O. Olsson, C.B.M. Andersson, M.C. Hakansson, J. Kanski, L. Ilver, U.O. Karlsson, *Phys. Rev. Lett.* 76 (1996) 3626.
- [19] S.P. Fu, T.J. Lin, W.S. Su, C.Y. Shieh, Y.F. Chen, C.A. Chang, N.C. Chen, P.H. Chang, *J. Appl. Phys.* 99 (2006) 126102.
- [20] J.C. Ho, P. Specht, Q. Yang, X. Xu, D. Hao, E.R. Weber, *J. Appl. Phys.* 98 (2005) 093712.
- [21] M. Drago, P. Vogt, W. Richter, *Phys. Stat. Sol. (a)* 203 (2006) 116.
- [22] L.F.J. Piper, T.D. Veal, P.H. Jefferson, C.F. McConville, F. Fuchs, J. Furthmuller, F. Bechstedt, H. Lu, W.J. Schaff, *Phys. Rev. B* 72 (2005) 245319.
- [23] M. Draxler, M. Walker, C.F. McConville, *Nucl. Instr. Meth. B* 249 (2006) 886.
- [24] D. Segev, C.G. Van de Walle, *Europhys. Lett.* 76 (2006) 305.
- [25] R.P. Bhatta, B.D. Thoms, M. Alevli, V. Woods, N. Dietz, *Appl. Phys. Lett.* 88 (2006) 122112.
- [26] V.J. Bellito, B.D. Thoms, D.D. Koleske, A.E. Wickenden, R.L. Henry, *Surf. Sci.* 430 (1999) 80.
- [27] H. Ibach, D.L. Mills, *Electron Energy Loss Spectroscopy and Surface Vibrations*, Academic, New York, 1982.
- [28] N. Nienhaus, S.P. Grabowski, W. Monch, *Surf. Sci.* 368 (1996) 196.
- [29] U.D. Pennino, C. Mariani, A. Ammoddeo, F. Proix, C. Sebenne, *J. Elect. Spectr. Rel. Phen.* 64 (1993) 491.
- [30] X. Hou, S. Yang, G. Dong, X. Ding, X. Wang, *Phys. Rev. B* 35 (1987) 8015.
- [31] J. Fritsch, A. Eckert, P. Pavone, U. Schroder, *J. Phys. Condens. Mat.* 7 (1995) 7717.
- [32] C.K. Gan, D.J. Srolovitz, *Phys. Rev. B* 74 (2006) 115319.
- [33] H. Froitzheim, H. Ibach, D.L. Mills, *Phys. Rev. B* 11 (1975) 4980.
- [34] P.J. Chen, J.E. Rowe, J.T. Yates Jr., *Phys. Rev. B* 50 (1994) 18134.